Research article

Tao He, Yukun Zhao, Xiaodong Zhang*, Wenkui Lin, Kai Fu, Chi Sun, Fengfeng Shi, Xiaoyu Ding, Guohao Yu, Kai Zhang, Shulong Lu, Xinping Zhang and Baoshun Zhang*

Solar-blind ultraviolet photodetector based on graphene/vertical Ga_2O_3 nanowire array heterojunction

https://doi.org/10.1515/nanoph-2018-0061
Received May 17, 2018; revised June 28, 2018; accepted July 18, 2018

Abstract: In this paper, a solar-blind ultraviolet photodetector (PD) based on the graphene/vertical Ga_2O_3 nanowire array heterojunction was proposed and demonstrated. To the best of our knowledge, it is the first time that vertical Ga_2O_3 nanowire arrays have been realized. Ga_2O_3 nanowires were obtained by thermally oxidizing GaN nanowires grown by molecular beam epitaxy on n-doped Si substrate. Then, a monolayer graphene film was transferred to Ga_2O_3 nanowires to form the graphene/vertical Ga_2O_3 nanowire array heterojunction and transparent electrodes. The fabricated device exhibited a responsivity (R) of 0.185 A/W and rejection ratio (R258 nm/R365 nm) of 3×10^4 at the bias of −5 V. Moreover, the fast response times of this PD were 9 and 8 ms for the rise and decay times under 254 nm illumination, respectively, which are attributed to the unique properties of nanowire arrays and the graphene/vertical Ga_2O_3 nanowire array heterojunction structure.

Keywords: graphene; heterojunction; photodetectors; thermal oxidation; vertical Ga_2O_3 nanowire arrays.

1 Introduction

With the rapidly increasing demand for solar-blind ultraviolet (UV) photodetectors (PDs) on various military and civilian applications, including flame sensors, missile interception, biological analysis, and UV radiation monitoring below the ozone hole, Ga_2O_3 with an ultrawide bandage of 4.9 eV is considered as a promising candidate for solar-blind detection [1–4]. Due to the unique structural and optical properties of nanowires, Ga_2O_3 nanowires can enhance the performance of solar-blind UV PDs [5–8]. The vertical nanowire array structures display more superior optical absorption ability, higher carrier generation, and higher recovery efficiency, resulting from high surface-to-volume ratio, surface carrier recombination, and effective optical coupling between the nanowire arrays and the incident light compared to thin films or flat disordered nanowires [9]. At present, some methods [e.g. vapor-liquid-solid mechanism, pulsed laser deposition (PLD), thermal evaporation, molecular beam epitaxy (MBE), and metal-organic chemical vapor deposition] have been used to grow Ga_2O_3 nanowires [10–13]. Guo et al. [11] grew vermicular Ga_2O_3 nanowire thin film by PLD and fabricated the metal-semiconductor-metal UV PDs. The rise and decay times of PDs under 254 nm illumination were estimated to be 4.3 and 8.4 s, respectively. Wu et al. [8] reported the growth of β-Ga_2O_3 nanowires using a vapor-phase transport method on

***Corresponding authors: Xiaodong Zhang and Baoshun Zhang,** Key Laboratory of Nanodevices and Applications, Suzhou Institute of Nano-Tech and Nano-Bionics, Chinese Academy of Sciences, Suzhou 215123, P.R. China, e-mail: xdzhang2007@sinano.ac.cn (X. Zhang); bszhang2006@sinano.ac.cn (B. Zhang)
Tao He and Xiaoyu Ding: School of Materials Science and Engineering, Nanjing University of Science and Technology, Nanjing 210094, P.R. China; and Key Laboratory of Nanodevices and Applications, Suzhou Institute of Nano-Tech and Nano-Bionics, Chinese Academy of Sciences, Suzhou 215123, P.R. China. http://orcid.org/0000-0003-3153-4390 (T. He)
Yukun Zhao, Wenkui Lin, Kai Fu, Chi Sun, Guohao Yu and Shulong Lu: Key Laboratory of Nanodevices and Applications, Suzhou Institute of Nano-Tech and Nano-Bionics, Chinese Academy of Sciences, Suzhou 215123, P.R. China
Fengfeng Shi: Key Laboratory of Nanodevices and Applications, Suzhou Institute of Nano-Tech and Nano-Bionics, Chinese Academy of Sciences, Suzhou 215123, P.R. China; and Department of Informatics, Beijing University of Technology, Beijing 100022, P.R. China
Kai Zhang: International Laboratory for Adaptive Bio-nanotechnology, Suzhou Institute of Nano-Tech and Nano-Bionics, Chinese Academy of Sciences, Suzhou 215123, P.R. China
Xinping Zhang: School of Materials Science and Engineering, Nanjing University of Science and Technology, Nanjing 210094, P.R. China

SiO_2/Si template. The fabricated β-Ga_2O_3 nanowire solar-blind PDs exhibited a responsivity of 3.43×10^{-3} A/W and response time in the order of seconds. However, the structures of nanowires in current reports on PDs based on Ga_2O_3 nanowires were mostly unordered or inclined, which cannot make full use of the effect of nanowires to improve the performance of solar-blind UV PDs. The epitaxial growth of vertical Ga_2O_3 nanowire arrays is very difficult to achieve and the construction of PDs based on vertical Ga_2O_3 nanowire arrays via a simple and feasible method is still a great challenge.

As it is well known, GaN or GaAs can be oxidized into Ga_2O_3 at high temperature in O_2, O_3, N_2O, or H_2O vapor ambient [14–17]. Huang et al. [18] investigated the realization of β-Ga_2O_3 thin film by simple furnace oxidation of GaN thin film and the fabrication of a solar-blind β-Ga_2O_3 PD with an extremely large deep UV-to-visible rejection ratio. In addition to the epitaxy technologies, thermal oxidation is also a feasible method to realize Ga_2O_3 nanowires.

In this work, vertical Ga_2O_3 nanowire arrays were prepared by thermally oxidizing GaN nanowires grown by MBE on n-doped Si substrate and a monolayer graphene film was transferred to Ga_2O_3 nanowires to form the graphene/Ga_2O_3 heterojunction and transparent electrodes. Based on the graphene/vertical Ga_2O_3 nanowire array heterojunction, solar-blind UV PDs with high performance were proposed and demonstrated. Meanwhile, the results showed that the graphene/vertical Ga_2O_3 nanowire array heterojunction structure realized by thermal oxidation might provide a new development direction of UV PDs based on Ga_2O_3.

2 Experiments

Vertical Ga_2O_3 nanowire arrays were obtained from GaN nanowires by thermal oxidization. First, vertical GaN nanowire arrays were grown along the (002) orientation on n-type Si substrate (resistivity 2–4 Ω cm) by MBE. Then, GaN nanowires were oxidized in a quartz tube purged with O_2 gas at 1000°C for 10 min after removing the native oxide layer of GaN nanowires by diluted hydrochloric acid-water solution. The rear SiO_2 layer on Si substrate formed during thermal oxidation was removed and Ti/Al (50/100 nm) was deposited by electron beam evaporation as the rear electrodes followed by rapid thermal annealing at 400°C for 30 min to form the ohmic contact. Then, a 200-nm-thick SiO_2 dielectric layer was deposited by inductively coupled plasma chemical vapor deposition at 75°C and selectively etched by reactive ion etching to expose Ga_2O_3 nanowires of square regions. After deposition, a monolayer graphene film was transferred to Ga_2O_3 nanowires to form the graphene/vertical Ga_2O_3 nanowire array heterojunction and transparent electrodes by wet transfer [19]. Finally, the proposed device was finished after the deposition of the front electrode (Ti/Au 50/200 nm). The specific fabrication process is shown in Figure 1.

The morphology and properties of the graphene were characterized by optical microscopy and micro-Raman spectroscopy (LABRAM HR, Horiba, Tokyo, Japan) with an Ar^+ laser (excitation wavelength 532 nm). The morphology of the nanowires was observed by field-emission scanning electron microscopy (FESEM; Hitachi S-4800, Hitachi, Tokyo, Japan) and high-resolution transmission electron

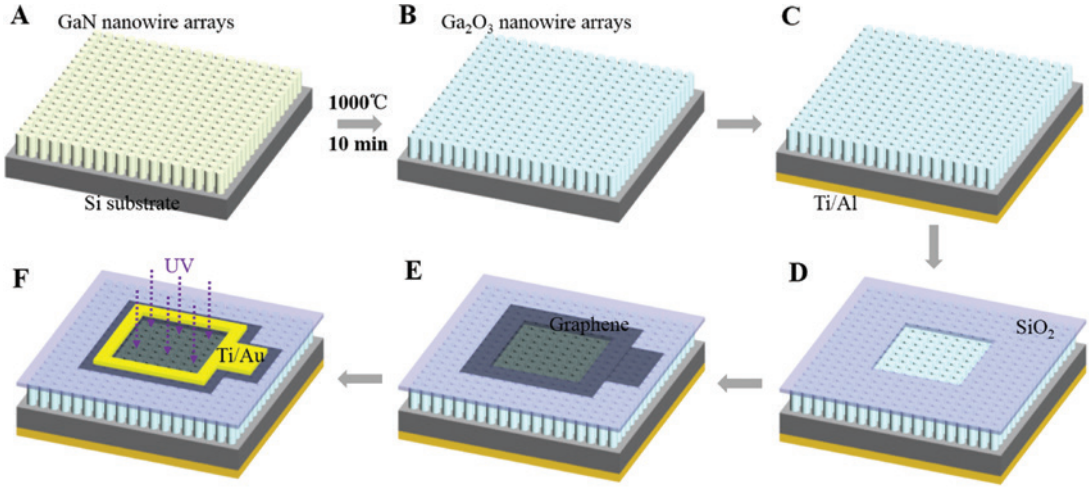

Figure 1: Schematic diagram of device fabrication.
(A) Growing GaN nanowire arrays on Si substrate, (B) preparing Ga_2O_3 nanowire arrays by thermal oxidation, (C) depositing the rear electrodes (Ti/Al), (D) depositing and selectively etching the SiO_2 dielectric layer, (E) transferring a monolayer graphene film to Ga_2O_3 nanowires, and (F) depositing the front electrodes (Ti/Au).

microscopy (HR-TEM; Tecnai G2 F20 S-TWIN, Thermo Fisher Scientific, Hillsboro, OR, USA). The elemental analysis of Ga_2O_3 nanowires on Si substrate was measured by energy-dispersive spectrometer (EDS; Quanta 400 FEG, Thermo Fisher Scientific, Hillsboro, OR, USA). The crystal structure was determined by X-ray diffraction (XRD; Bruker D8 Advance, Bruker, Karlsruhe, Germany). The current-voltage (*I-V*) and transient responses characteristics of PDs were measured by Agilent B1505A, Agilent, Santa Clara, CA, USA. The spectral response characteristics were measured with the photoelectric measurement system consisting mainly of mercury lamp, optical chopper, phase-locked, and power supply.

3 Results and discussion

Figure 2A depicts the Raman spectrum of the monolayer graphene film and the inset is the optical microscopy image of the graphene/SiO_2/Ga_2O_3 nanowire structure. A strong G peak (1594 cm^{-1}) and 2D peak (2694 cm^{-1}) with the Raman intensity ratio of $I_{2D}/I_G = 2.3$ are detected. The defect related D peak is barely visible, confirming the high crystal quality of the monolayer graphene film.

FESEM images of vertical GaN nanowire arrays on Si substrate before and after thermal oxidization are shown in Figure 2B and C, respectively. After thermal oxidization, the diameter of the oxidized nanowires increases by approximately 10 nm, but height has nearly no change. It should be noted that the oxidized nanowires are slightly curved, which could be attributed to GaN decomposition at high temperatures. The HR-TEM image of the partial enlargement of oxidized nanowires (Figure 2D) demonstrates that the oxidized nanowires are polycrystalline with good crystallinity and large grains. The spacing between two parallel fringes is approximately 0.368 nm corresponding to the interplanar distance of (201) lattice planes of monoclinic β-Ga_2O_3. To further determine whether the oxidized nanowires are Ga_2O_3 or not, the EDS spectrum (Figure 2E) is extracted from the oxidized sample. The Si signal from the substrate at 1.7 keV has been removed to make other signals more visible. Only Ga, O, and C signals are observed in the spectrum, where the small amount of C signal should be related to contamination. It implies that GaN nanowires have been totally oxidized into Ga_2O_3 nanowires. In the meantime, XRD patterns (Figure 2F) of vertical GaN nanowire arrays on Si (111) substrate before and after thermal oxidation also attest to this result. The GaN (002) peak

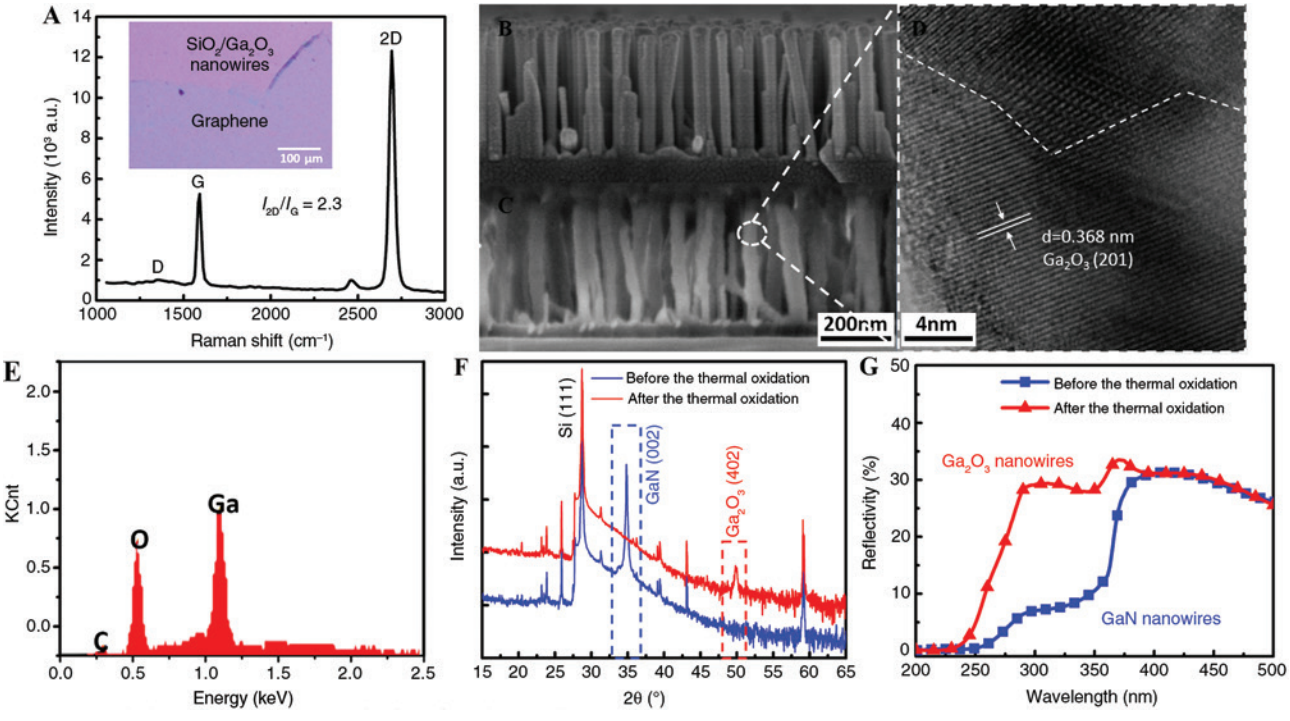

Figure 2: Morphology and optical characterization of graphene and nanowire arrays.
(A) Raman spectrum of the monolayer graphene film with the optical microscopy image of graphene and SiO_2/Ga_2O_3 nanowire structure in inset. (B and C) FESEM images of vertical GaN and Ga_2O_3 nanowire arrays. (D) HR-TEM image of Ga_2O_3 nanowires. (E) EDS diffraction spectra of vertical Ga_2O_3 nanowire arrays on Si substrate. Si signal from the substrate at 1.7 keV has been removed to make other signals more visible. (F and G) XRD patterns and reflection spectra of vertical GaN nanowire arrays before and after thermal oxidation.

disappears and a new Ga_2O_3 peak appears at 49.84° after thermal oxidation. This new diffraction peak is assigned as (402) planes of β-Ga_2O_3 with monoclinic structure (JCPDS Card No. 43-1012), which could be the preferred orientation in the growth process of Ga_2O_3 nanowires. As mentioned above, because grown Ga_2O_3 nanowires are polycrystalline with some defects and grain boundaries, the intensity of the Ga_2O_3 (402) peak is weak. In addition, Figure 2G shows the reflection spectra of vertical GaN nanowire arrays on Si substrate before and after thermal oxidization, in which the light reflectivity of Ga_2O_3 and GaN nanowires is observed to decrease when the wavelength is reduced to 281 and 366 nm, corresponding to their cutoff absorption edges, respectively [20, 21]. The decrease in reflectivity of Ga_2O_3 nanowires at 281 nm is attributed to Ga^{3+} vacancies in the conduction band [20]. To the best of our knowledge, it is the first time that vertical Ga_2O_3 nanowire arrays have been realized by thermal oxidation. However, lattice mismatch and built-in stress cause the appearance of defects and grain boundaries in Ga_2O_3 nanowires during thermal oxidation. The defects and grain boundaries in Ga_2O_3 nanowires can adversely affect the performance of PDs. When UV illumination is irradiated on Ga_2O_3 nanowires, the defects and grain boundaries can trap photogenerated carriers, which can reduce the photocurrent and responsivity of the device. In addition, the capture and release of photogenerated carriers caused by the defects and grain boundaries in Ga_2O_3 nanowires can reduce the response speed and increase the response time of PDs. The improvement of crystal quality of Ga_2O_3 nanowire is a matter of future investigations to enhance the performance of PDs.

To check the solar-blind UV photoresponse of PDs, *I-V* characteristics should be measured. As monolayer graphene allows 90 T% (transmission rate) of the incident light in the range of 200 to 1000 nm, UV light could easily penetrate and irradiate on the heterojunction, enhancing the light harvesting [22]. Figure 3 exhibits the *I-V* curves of PDs under dark. It is obvious that nonlinear *I-V* characteristics can be used as a reflection of the rectifying characteristics ascribed to the graphene/vertical Ga_2O_3 nanowire array heterojunction. The rectifying ratio ($I_{1\ V}/I_{-1\ V}$) is over 10^2 with no illumination and the dark current is 1.14 μA at –1 V. Moreover, further analysis has been performed on PDs by fitting the equation, which is described as [23]

$$I = I_0\left[\exp\left(\frac{qV}{nkT}\right)-1\right] \quad (1)$$

$$I_0 = SA\star T^2\exp\left(\frac{-\phi_B}{kT}\right) \quad (2)$$

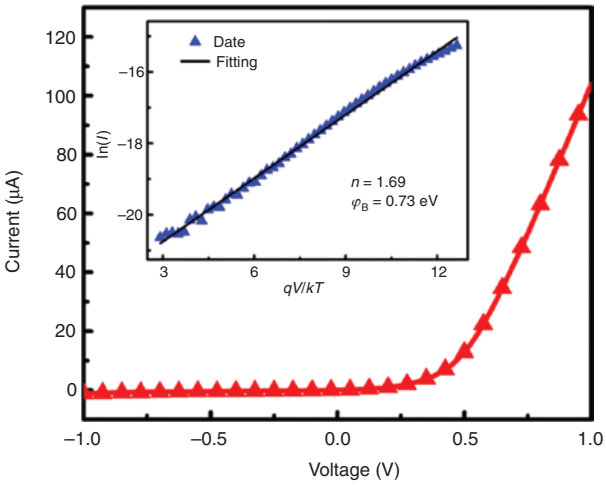

Figure 3: *I-V* characteristics of PD measured at room temperature under dark.
(Inset) ln(*I*) vs. qV/kT used to estimate n and ϕ_B at the graphene/Ga_2O_3 heterojunction.

where I_0 is the saturation current, $A^\star$ is the modified Richardson constant for semiconductor, S is the contact area, n is the diode ideality factor, ϕ_B is the barrier height, q is the fundamental electric charge, k is the Boltzmann constant, and T is the absolute temperature. The $A^\star$ value used in this analysis is estimated to be 41 A $cm^{-2}\cdot K^{-2}$ using the electron effective mass of 0.342 m_0 at room temperature. Under forward bias, the above equation can be rearranged to extract the n and ϕ_B as shown in Figure 3 (inset). Accordingly, n and ϕ_B are estimated at values of 1.69 and 0.67 eV, respectively. These values are comparable to previously reported results for graphene/Ga_2O_3 heterojunction [24].

To quantitatively assess the device performance of PDs, the responsivity defined as the photocurrent generated per unit power of the incident light on the effective area of the PD is calculated [1]. From the spectral response of PDs, (Figure 4), the PD shows a peak responsivity of 0.185 and 0.029 A/W at 258 nm wavelength at the bias of –5 and –3 V, respectively. The ratio of the photo-dark current is 57.2 and the rejection ratio ($R_{258\ nm}/R_{365\ nm}$) of the device is about 3×10^4 at –5 V, which illustrates the strong selectivity of PD to the solar-blind UV. Figure 5A and B displays the transient response of PDs based on the graphene/vertical Ga_2O_3 nanowire array heterojunction to 254 nm illumination at –5 V, from which both the rising time (τ_{on}, defined as the time during which the current rises to the waveform's maximum height) and the decay time (τ_{off}, defined as the time during which the current decreases to the base line) are extracted. As shown in Figure 5B, the device exhibits fast response times (9 and 8 ms for τ_{on} and τ_{off}, respectively) superior to some reported

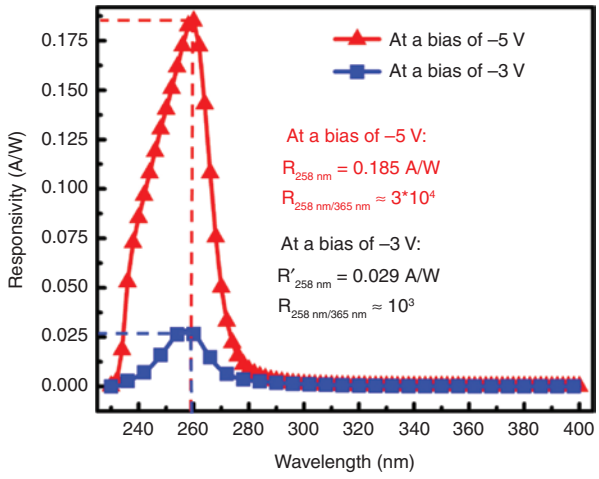

Figure 4: Spectral response of PDs based on the graphene/vertical Ga_2O_3 nanowire array heterojunction at the bias of –3 and –5 V.

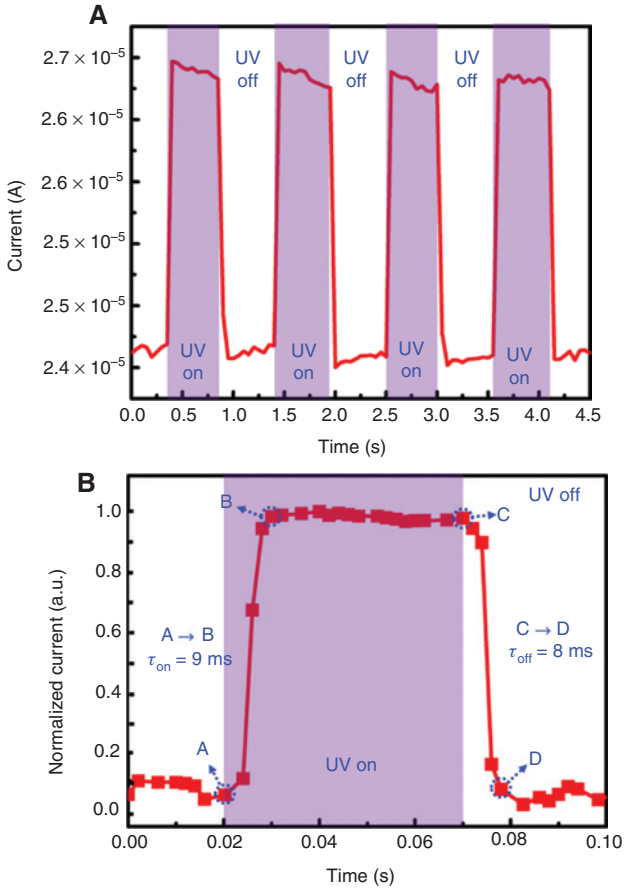

Figure 5: Transient response of PDs to 254 nm illumination at the bias of –5 V.
(A) Response for multicycles and (B) normalized response on a linear scale.

values [8, 11, 25–28]. The improvement of the response time may be attributed to two factors [29]: (i) the property of Ga_2O_3 nanowires and (ii) the heterojunction structure

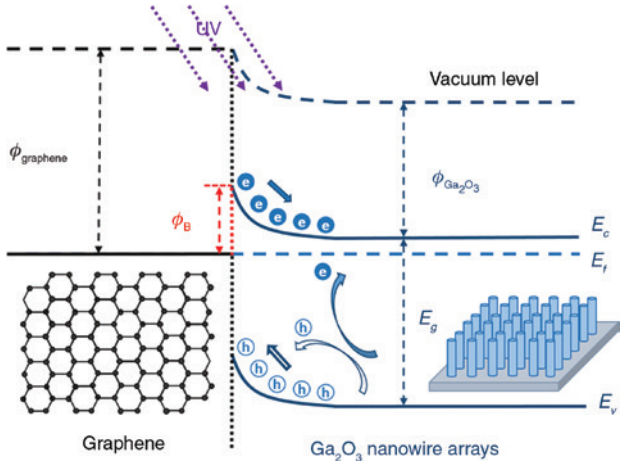

Figure 6: Energy band diagram of the graphene/Ga_2O_3 nanowire array heterojunction at UV illumination.

between graphene and Ga_2O_3 nanowires. Compared to Ga_2O_3 thin films, vertical Ga_2O_3 nanowire arrays have higher surface-to-volume ratio and surface carrier recombination, which leads to much higher carrier generation and recovery efficiency. Besides, the heterojunction structure between graphene and Ga_2O_3 nanowires also contributes to the fast response time of PDs. Figure 6 illustrates an energy band diagram of the graphene/Ga_2O_3 nanowire array heterojunction. When UV illumination is irradiated on PDs, Ga_2O_3 nanowires absorb the photons and the electrons in the valence band are inspired to the conduction band, leading to the generation of electron-hole pairs. Then, photogenerated electron-hole pairs in the depletion region caused by the upwardly bended energy band are separated quickly. After turning off the UV illumination, the electron-hole pairs recombine very rapidly under the influence of the heterojunction structure.

4 Conclusion

In conclusion, a solar-blind UV PD based on the graphene/vertical Ga_2O_3 nanowire array heterojunction was demonstrated and vertical Ga_2O_3 nanowire arrays were realized by thermally oxidizing GaN nanowires grown by MBE on n-doped Si substrate for the first time. The fabricated device exhibited the large rejection ratio (R258 nm/R365 nm) of 3×104 and responsivity of 0.185 A/W at the bias of –5 V. Furthermore, thanks to the nanowire structure and heterojunction between graphene and Ga_2O_3 nanowires, the improved rise and decay times were 9 and 8 ms under 254 nm illumination, respectively. These results indicate that PDs based on the graphene/vertical

Ga_2O_3 nanowire array heterojunction realized by thermal oxidation might open up new possibilities for future optoelectronic systems.

Acknowledgments: This work was supported by the National Natural Science Foundation of China (grant no. 61704185) and the Key Research and Development Program of Jiangsu Province (grant no. be2016084).

References

[1] Assefa S, Xia F, Vlasov YA. Reinventing germanium avalanche photodetector for nanophotonic on-chip optical interconnects. Nature 2010;464:80.
[2] Oh S, Kim CK, Kim J. High responsivity β-Ga_2O_3 metal-semiconductor-metal solar-blind photodetectors with ultraviolet transparent graphene electrodes. ACS Photonics 2018;5:1123–8.
[3] Razeghi M. Short-wavelength solar-blind detectors-status, prospects, and markets. Proc IEEE 2002;90:1006–14.
[4] Orita M, Ohta H, Hirano M, Hosono H. Deep-ultraviolet transparent conductive β-Ga_2O_3 thin films. Appl Phys Lett 2000;77:4166–8.
[5] Tian W, Zhi CY, Zhai TY, et al. In-doped Ga_2O_3 nanobelt based photodetector with high sensitivity and wide-range photoresponse. J Mater Chem 2012;22:17984.
[6] Chen PH, Hsieh CH, Chen SY, et al. Direct observation of Au/Ga_2O_3 peapodded nanowires and their plasmonic behaviors. Nano Lett 2010;10:3267–71.
[7] Hsieh CH, Chou LJ, Lin GR, Bando Y, Golberg D. Nanophotonic switch: gold-in-Ga_2O_3 peapod nanowires. Nano Lett 2008;8:3081–5.
[8] Wu YL, Chang SJ, Weng WY, et al. Ga_2O_3 nanowire photodetector prepared on SiO_2/Si template. IEEE Sens J 2013;13:2368–73.
[9] Tian BZ, Zheng XL, Kempa TJ, et al. Coaxial silicon nanowires as solar cells and nanoelectronic power sources. Nature 2007;449:885.
[10] Nguyen TD, Kim ET, Dao KA. Ag nanoparticle catalyst based on Ga_2O_3/GaAs semiconductor nanowire growth by VLS method. J Mater Sci Mater Electron 2015;26:8747–52.
[11] Guo DY, Wu ZP, Li PG, et al. Magnetic anisotropy and deep ultraviolet photoresponse characteristics in Ga_2O_3: Cr vermicular nanowire thin film nanostructure. RSC Adv 2015;5:12894–8.
[12] Cao CB, Chen Z, An XQ, Zhu HS. Growth and field emission properties of cactus-like gallium oxide nanostructures. J Phys Chem C 2008;112:95–8.
[13] Han WQ, Kohler-Redlich P, Ernst F, Rühle M. Growth and microstructure of Ga_2O_3 nanorods. Solid State Commun 2000;115:527–9.
[14] Kim H, Park SJ, Hwang H. Thermally oxidized GaN film for use as gate insulators. J Vac Sci Technol B Microelectron Nanomet Struct 2001;19:579.
[15] Weng WY, Hsueh TJ, Chang SJ, Huang GJ, Hsueh HT. A β-Ga_2O_3 solar-blind photodetector prepared by furnace oxidization of GaN thin film. IEEE Sens J 2011;11:999–1003.
[16] Oon HS, Cheong KY. Recent development of gallium oxide thin film on GaN. Mater Sci Semicond Process 2013;16:1217–31.
[17] Oon HS, Cheong KY. Effect of oxidation time on thermally grown oxide on GaN. J Mater Eng Perform 2013;22:1341–7.
[18] Huang ZD, Weng WY, Chang SJ, Chiu CJ, Hsueh TJ, Wu SL. Ga_2O_3/AlGaN/GaN heterostructure ultraviolet three-band photodetector. IEEE Sens J 2013;13:3462–7.
[19] Zhang K, Zhang L, Yap FL, Song P, Qiu CW, Loh KP. Large-area graphene nanodot array for plasmon-enhanced infrared spectroscopy. Small 2016;12:1302–8.
[20] Dong LP, Jia RX, Xin B, Peng B, Zhang YM. Effects of oxygen vacancies on the structural and optical properties of β-Ga_2O_3. Sci Rep 2017;7:1–12.
[21] Choi MK, Kim GS, Jeong JT, et al. Functionalized vertical GaN micro pillar arrays with high signal-to-background ratio for detection and analysis of proteins secreted from breast tumor cells. Sci Rep 2017;7:1–12.
[22] Lee HC, Liu WW, Chai SP, et al. Review of the synthesis, transfer, characterization and growth mechanisms of single and multilayer graphene. RSC Adv 2017;7:15644–93.
[23] Sharma BL. Metal-semiconductor Schottky barrier junctions and their applications. New York, Plenum Press, 1984.
[24] Yao Y, Gangireddy R, Kim J, et al. Electrical behavior of β-Ga_2O_3 Schottky diodes with different Schottky metals. J Vac Sci Technol B 2017;35:03D113.
[25] Guo DY, Shi HY, Qian YP, et al. Fabrication of β-Ga_2O_3/ZnO heterojunction for solar-blind deep ultraviolet photodetection. Semicond Sci Technol 2017;32:03LT01.
[26] Ai ML, Guo DY, Qu YY, et al. Fast-response solar-blind ultraviolet photodetector with a graphene/β-Ga_2O_3/graphene hybrid structure. J Alloys Compd 2017;692:634–8.
[27] Qu YY, Wu ZP, Ai ML, et al. Enhanced Ga_2O_3/SiC ultraviolet photodetector with graphene top electrodes. J Alloys Compd 2016;680:247–51.
[28] Yu FP, Ou SL, Wuu DS. Pulsed laser deposition of gallium oxide films for high performance solar-blind photodetectors. Opt Mater Express 2015;5:1240–9.
[29] Fu XW, Liao ZM, Zhou YB, et al. Graphene/ZnO nanowire/graphene vertical structure based fast-response ultraviolet photodetector. Appl Phys Lett 2012;100:22311.